PUBLIC HEALTH

Early-life exposure to tobacco, genetic susceptibility, and accelerated biological aging in adulthood

Feipeng Cui[1,2], Linxi Tang[1,2], Dankang Li[1,2], Yudiyang Ma[1,2], Jianing Wang[1,2], Junqing Xie[3], Binbin Su[4]*, Yaohua Tian[1,2]*, Xiaoying Zheng[4]*

Early-life tobacco exposure serves as a non-negligible risk factor for aging-related diseases. To understand the underlying mechanisms, we explored the associations of early-life tobacco exposure with accelerated biological aging and further assessed the joint effects of tobacco exposure and genetic susceptibility. Compared with those without in utero exposure, participants with in utero tobacco exposure had an increase in Klemera-Doubal biological age (KDM-BA) and PhenoAge acceleration of 0.26 and 0.49 years, respectively, but a decrease in telomere length of 5.34% among 276,259 participants. We also found significant dose-response associations between the age of smoking initiation and accelerated biological aging. Furthermore, the joint effects revealed that high–polygenic risk score participants with in utero exposure and smoking initiation in childhood had the highest accelerated biological aging. There were interactions between early-life tobacco exposure and age, sex, deprivation, and diet on KDM-BA and PhenoAge acceleration. These findings highlight the importance of reducing early-life tobacco exposure to improve healthy aging.

INTRODUCTION

Biological aging is a complex and progressively deteriorating process in the multisystem, which originates from cumulative changes at the cellular level and gradually destroys the integrity and resilience of tissues and organs over time (*1*). With the dramatic increase in the global population aging, accelerated aging drives adults more vulnerable to morbidity and mortality, leading to a rapid growth in the financial burden of aging-related health care (*2*, *3*). Recently, two reviews have summarized that biological age (BA) can be quantified using telomere length (TL), epigenetic, transcriptomic, proteomic, metabolomic, and composite clinical-parameter algorithms across the dimensions of molecular, cellular, organ, and systemic levels (*4*, *5*). Among them, the composite clinical-parameter algorithms have been found to accurately predict morbidity and mortality (*6*, *7*). Of note, individuals with the same chronological age (CA) may have different BAs and susceptibility to age-related disorders (*8*). It is critical to identify the determinants of accelerated biological aging to develop preventive and therapeutic interventions aimed at reversing the biological clocks and extending both life span and health span.

The Developmental Origins of Health and Disease hypothesis proposed that early life was the sensitive or critical window of vulnerability to exposure (*9*). During this period, environmental exposure permanently altered the body's structure, metabolism, and physiology, leading to adverse outcomes in later childhood and adult life (*10*). Growing evidence showed that early-life tobacco exposures, including the fetal period, childhood, and adolescence, were recognized as the significant risk factors for multiple adverse outcomes in adulthood, such as chronic obstructive pulmonary disease (*11*), type 2 diabetes (*12*), cardiovascular disease (CVD) (*13*), cancer (*14*), and mortality (*15*). Considering that CA is a major factor that increases the risk of chronic diseases and death in later life, it follows that early-life tobacco exposure may accelerate the biological aging process and subsequently render individuals more vulnerable to chronic diseases. Several studies documented that tobacco exposure during pregnancy and childhood was associated with shortened TL among fetuses and children and accelerated epigenetic aging in childhood (*16*–*19*). However, these studies focused on biological aging in early life. To date, only one study has explored the association of smoking in youth with epigenetic aging in adults over 50 years old (*20*). The effects of smoking during other periods, such as the fetal period, as well as the age of smoking initiation, on biological aging in adulthood, remain unknown.

Apart from environmental exposure, genetic susceptibility also plays a vital role in biological aging (*21*). Multiple large-scale genome-wide association studies have identified numerous genetic variants associated with BA (*22*, *23*). On the basis of these findings, researchers have constructed polygenic risk scores (PRS) as a potential tool to predict an individual's genetic susceptibility to specific outcomes related to BA (*24*, *25*). Additionally, previous studies have evaluated the interplay between early-life tobacco exposure and PRS (*12*, *14*), but no studies have elucidated the role that genetic susceptibility played in the relationships between early-life tobacco exposure and biological aging in adulthood.

Given that a single biomarker did not depict the whole landscape of the biological aging process (*5*, *21*), we applied multiple dimensions of biological aging biomarkers, including TL and two BAs validated in the UK Biobank, to examine the associations between early-life tobacco exposure and accelerated biological aging in adulthood. Furthermore, we comprehensively explored the potential joint and interaction effects of genetic susceptibility and early-life tobacco exposure on accelerated biological aging.

[1]Key Laboratory of Environment and Health, Ministry of Education & Ministry of Environmental Protection, and State Key Laboratory of Environmental Health (incubating), School of Public Health, Tongji Medical College, Huazhong University of Science and Technology, Wuhan, Hubei, PR China. [2]Department of Maternal and Child Health, School of Public Health, Tongji Medical College, Huazhong University of Science and Technology, No. 13 Hangkong Road, Wuhan 430030, Hubei, PR China. [3]Center for Statistics in Medicine, NDORMS, University of Oxford, The Botnar Research Centre, Oxford, UK. [4]School of Population Medicine and Public Health, Chinese Academy of Medical Sciences/Peking Union Medical College, No. 31, Beijige-3, Dongcheng District, Beijing 100730, PR China.
*Corresponding author. Email: subinbin@sph.pumc.edu.cn (B.S.); yaohua_tian@hust.edu.cn (Y.T.); zhengxiaoying@sph.pumc.edu.cn (X.Z.)

RESULTS

Baseline characteristics of participants

Table S1 compares the characteristics of the total population and included participants. There were similar characteristics among the three groups. The characteristics of the analytic participants across early-life tobacco exposure are summarized in Table 1. Compared to those without in utero tobacco exposure, participants with in utero exposure were slightly younger, more likely to be males and drinkers, and had higher body mass index (BMI) and Townsend deprivation index (TDI), unhealthy diet, higher prevalence of major diseases, and accelerated biological aging, which was generally consistent with the results in participants with early initiation of smoking. At baseline, CA, Klemera-Doubal BA (KDM-BA), and PhenoAge were strongly correlated with each other (Pearson coefficient ranged from 0.84 to 0.88), while age acceleration indicators were not correlated with CA (fig. S1).

Association of early-life tobacco exposure with accelerated biological aging

Table 2 shows the associations between early-life tobacco exposure with accelerated biological aging. Compared with participants without in utero tobacco exposure, those with in utero exposure had an increase in KDM-BA and PhenoAge acceleration [0.26 years; 95% confidence interval (CI): 0.24 to 0.29 for KDM-BA; 0.49 years; 95% CI: 0.44, 0.53 for PhenoAge] but had a decrease in TL (−5.34%; 95% CI: −6.10%, −4.58%) after adjusting for model 2. Significant dose-response associations between the age of smoking initiation and accelerated biological aging were observed (all $P_{trend} < 0.001$). In comparison with never-smokers, childhood exposure to tobacco was associated with 0.88- and 2.51-year increases in KDM-BA and PhenoAge acceleration, respectively, and 10.53% decreases in TL. The effect of exposure on PhenoAge acceleration was stronger than that on KDM-BA acceleration (table S2). Effect estimates were similar in a series of sensitivity analyses (tables S3 to S6). When analyzing the combined effects of in utero tobacco exposure and the age of smoking initiation, participants with in utero exposure and smoking initiation in childhood had the highest accelerated biological aging [KDM-BA acceleration: 1.13 (1.04, 1.21) years; PhenoAge acceleration: 2.89 (2.75, 3.03) years; TL: −14.41% (−16.55%, −12.21%)] (Fig. 1).

Joint effect of genetic susceptibility and early-life tobacco exposure

We observed that PRS for KDM-BA, PhenoAge, and TL was significantly associated with accelerated biological aging (all $P_{trend} < 0.001$, table S7). Furthermore, we explored the joint effect of the three PRS and in utero exposure to tobacco smoke on accelerated biological aging (Fig. 2). Compared to those with low PRS and without in utero exposure, participants with high PRS and in utero exposure had the highest accelerated biological aging [KDM-BA acceleration: 0.45 (0.41, 0.50) years; PhenoAge acceleration: 1.99 (1.91, 2.07) years; TL: −26.96% (−28.03%, −25.88%)]. Similarly, individuals with smoking initiation in childhood and high PRS (low PRS and never-smokers as reference) had increased KDM-BA and PhenoAge acceleration of 1.08 (0.98, 1.18) and 4.07 (3.92, 4.23) years, respectively, and decreased TL of 30.6% (28.53%, 32.62%). The joint effects showed that individuals with in utero exposure, high PRS, and smoking initiation in childhood had the highest accelerated biological aging [KDM-BA acceleration: 1.39 (1.25, 1.54) years; PhenoAge acceleration: 4.28 (4.04, 4.52) years; TL: −34.27% (−37.26%, −31.13%)] (Fig. 3). However, no significant interaction was found between early-life tobacco exposure and PRS on accelerated biological aging ($P_{interaction} > 0.05$).

Stratified analyses

We performed a series of stratified analyses according to characteristics (tables S8 and S9). Significant modification effects between early-life tobacco exposures and age, sex, TDI, and healthy diet score on KDM-BA and PhenoAge acceleration were found (all $P_{interaction} < 0.05$). For example, compared with those without in utero tobacco exposure, younger participants (aged ≤50 years old) who were exposed to tobacco in utero had 0.38 (0.33, 0.43) years in KDM-BA acceleration, 0.69 (0.61, 0.78) years in PhenoAge acceleration, and −6.28% (−7.72%, −4.81%) in TL. In addition, there were stronger effects of in utero tobacco exposure on shortened TL in participants with high deprivation [−6.23% (−7.30%, −5.15%)] than in those with low deprivation [−4.33% (−5.41%, −3.25%)] ($P_{interaction} < 0.05$). Similarly, we also observed significant interactions between the age of smoking initiation and TDI on TL ($P_{interaction} < 0.05$).

DISCUSSION

This study explores the association between early-life tobacco exposure, including fetal periods, childhood, and adolescence, and accelerated biological aging in adulthood. In this large-scale study, we found that in utero exposure to tobacco smoke and the age of smoking initiation were pronouncedly associated with KDM-BA and PhenoAge acceleration, and shortened TL. Participants with in utero exposure, high PRS, and smoking initiation in childhood had the highest accelerated biological aging. There were interactions between early-life tobacco exposure and age, sex, TDI, and healthy diet on KDM-BA and PhenoAge acceleration. These findings from a large biobank cohort highlight the importance of reducing tobacco exposure in early life.

With the rapid growth of aging-related diseases, much effort has been made on the heterogeneity of biological aging of peers, in which tobacco exposure plays a non-negligible role (*20*, *26*, *27*). We found that early-life tobacco exposure was pronouncedly associated with shortened TL. In support of our results, an American birth cohort study found a positive association of intrauterine tobacco exposure with shortened fetal TL (*16*). Similar findings were also observed in children from the Hong Kong Child Health Survey and the Human Early-Life Exposome (HELIX) project (*17*, *18*). Prenatal smoking exposure among 408 extremely premature infants accelerated placental epigenetic gestational aging by 0.5 weeks (*28*). In our study, participants with in utero tobacco exposure had increased KDM-BA and PhenoAge acceleration by 0.26 and 0.49 years, which was comparable to the results from the Viva project, which showed that prenatal smoking exposure was associated with a 0.34-year increase in skin and blood epigenetic age acceleration among 120 children (*29*). Another study of 1173 children from the HELIX project reported that maternal smoking during pregnancy accelerated epigenetic aging by 0.14 years (*19*). Nevertheless, it was worth noting that this estimated effect was lower than our estimates. The discrepancy in the study design, sample size, demographic characteristics, and aging biomarkers may be responsible for the variation in biological aging effects. Previous studies have shown that the prevalence of smoking among pregnant women in Europe was 8.1%, and there were at least 50 million smokers aged ≤14 years (*14*, *30*). We

Table 1. Characteristics of study participants according to in utero exposure to tobacco smoke and age of smoking initiation. Mean values (standard deviation) for continuous variables and *n* (%) for categorical variables.

	In utero exposure to tobacco smoke (*n* = 276,259)			Age of smoking initiation (*n* = 275,844)				
Characteristics	**No (*n* = 195,773)**	**Yes (*n* = 80,486)**	***P***	**Never-smokers (*n* = 175,908)**	**Adulthood (>18 years) (*n* = 40,948)**	**Adolescence (15–18 years) (*n* = 43,184)**	**Childhood (5–14 years) (*n* = 15,804)**	***P***
Age at recruitment (years)	56.38 ± 8.27	55.90 ± 7.75	<0.001	55.74 ± 8.14	57.94 ± 7.95	57.62 ± 7.69	55.51 ± 8.00	<0.001
Sex (female)	107,519 (54.9)	42,667 (53.0)	<0.001	103,144 (58.6)	21,234 (51.9)	19,089 (44.2)	5,461 (34.6)	<0.001
Body mass index (BMI, kg/m^2)	27.08 ± 4.60	27.86 ± 4.88	<0.001	27.10 ± 4.70	27.53 ± 4.72	27.92 ± 4.63	28.56 ± 4.99	<0.001
Missing	396 (0.2)	152 (0.2)		369 (0.2)	83 (0.2)	85 (0.2)	44 (0.3)	
Ethnicity (white)	181,366 (92.6)	79,107 (98.3)	<0.001	164,369 (93.4)	38,950 (95.1)	42,142 (97.6)	15,330 (97.0)	<0.001
Missing	650 (0.3)	237 (0.3)		567 (0.3)	177 (0.4)	120 (0.3)	66 (0.4)	
Townsend deprivation index (TDI)	−1.47 ± 3.00	−1.23 ± 3.08	<0.001	−1.66 ± 2.89	−0.97 ± 3.19	−0.99 ± 3.18	−0.27 ± 3.41	<0.001
Missing	247 (0.1)	103 (0.1)		213 (0.1)	39 (0.1)	43 (0.1)	31 (0.2)	
Drinking status								
Never	10,179 (5.2)	2,221 (2.8)	<0.001	11,170 (6.3)	815 (2.0)	733 (1.7)	263 (1.7)	<0.001
Previous	6,231 (3.2)	3,018 (3.7)		4,938 (2.8)	1,752 (4.3)	1,962 (4.5)	944 (6.0)	
Current	179,152 (91.5)	75,174 (93.4)		159,625 (90.7)	38,332 (93.6)	40,452 (93.7)	14,571 (92.2)	
Missing	211 (0.1)	73 (0.1)		175 (0.1)	49 (0.1)	37 (0.1)	26 (0.2)	
Physical activity (MET, min/week)	2,621.84 ± 2,646.03	2,765.12 ± 2,844.79	<0.001	2,612.22 ± 2,628.48	2,581.95 ± 2,653.36	2,775.31 ± 2,885.28	3,012.30 ± 3,287.57	<0.001
Missing	35,884 (18.3)	14,168 (17.6)		33,239 (18.9)	7,270 (17.8)	8,481 (19.6)	3,152 (19.9)	
Healthy diet score								
0–1	42,143 (21.5)	18,941 (23.5)	<0.001	37,156 (21.1)	9,362 (22.9)	11,207 (26.0)	4,870 (30.8)	<0.001
2–3	123,813 (63.2)	50,424 (62.6)		112,536 (64.0)	25,437 (62.1)	26,274 (60.8)	8,905 (56.3)	
4–5	26,150 (13.4)	9,775 (12.1)		23,064 (13.1)	5,391 (13.2)	4,748 (11.0)	1,556 (9.8)	
Missing	3,667 (1.9)	1,346 (1.7)		3,152 (1.8)	758 (1.9)	955 (2.2)	473 (3.0)	
Birthplace (England)	153,460 (78.4)	67,118 (83.4)	<0.001	140,288 (79.8)	31,856 (77.8)	36,214 (83.9)	13,127 (83.1)	<0.001
Missing	348 (0.2)	34 (0.0)		294 (0.2)	45 (0.1)	21 (0.0)	17 (0.1)	
Body sizes at age 10 years								
Thinner	63,630 (32.5)	26,992 (33.5)	<0.001	57,100 (32.5)	12,750 (31.1)	14,028 (32.5)	5,500 (34.8)	<0.001
About average	100,073 (51.1)	38,245 (47.5)		89,028 (50.6)	20,790 (50.8)	21,425 (49.6)	7,222 (45.7)	
Plumper	28,434 (14.5)	14,214 (17.7)		26,220 (14.9)	6,683 (16.3)	6,983 (16.2)	2,796 (17.7)	
Missing	3,636 (1.9)	1,035 (1.3)		3,560 (2.0)	725 (1.8)	748 (1.7)	286 (1.8)	
Height sizes at age 10 years								
Shorter	37,778 (19.3)	17,863 (22.2)	<0.001	35,519 (20.2)	7,938 (19.4)	8,591 (19.9)	3,388 (21.4)	<0.001
About average	105,197 (53.7)	41,756 (51.9)		93,978 (53.4)	21,561 (52.7)	23,569 (54.6)	8,189 (51.8)	
Taller	49,509 (25.3)	19,786 (24.6)		43,020 (24.5)	10,822 (26.4)	10,323 (23.9)	3,954 (25.0)	
Missing	3,289 (1.7)	1,081 (1.3)		3,391 (1.9)	627 (1.5)	701 (1.6)	273 (1.7)	
Air pollution								
NO_2 (μg/m^3)	29.10 ± 9.27	28.92 ± 8.76	<0.001	28.60 ± 8.84	30.10 ± 9.92	29.14 ± 8.77	30.06 ± 8.87	<0.001
Missing	2,558 (1.3)	1,007 (1.3)		2,019 (1.1)	672 (1.6)	570 (1.3)	233 (1.5)	
NO_x (μg/m^3)	43.68 ± 15.59	44.14 ± 15.29	<0.001	43.13 ± 15.04	45.22 ± 16.46	44.55 ± 15.57	46.39 ± 16.29	<0.001
Missing	2,558 (1.3)	1,007 (1.3)		2,019 (1.1)	672 (1.6)	570 (1.3)	233 (1.5)	
$PM_{2.5}$ (μg/m^3)	9.96 ± 1.05	10.01 ± 1.06	<0.001	9.92 ± 1.03	10.07 ± 1.10	10.04 ± 1.07	10.17 ± 1.08	<0.001
Missing	9,626 (4.9)	4,195 (5.2)		8,594 (4.9)	2,308 (5.6)	2,090 (4.8)	821 (5.2)	
PM_{10} (μg/m^3)	19.33 ± 1.96	19.26 ± 1.88	<0.001	19.23 ± 1.91	19.50 ± 2.04	19.33 ± 1.87	19.48 ± 1.86	<0.001
Missing	10,022 (5.1)	4,419 (5.5)		8,970 (5.1)	2,397 (5.9)	2,189 (5.1)	870 (5.5)	

(Continued)

(Continued)

Characteristics	In utero exposure to tobacco smoke (n = 276,259)			Age of smoking initiation (n = 275,844)				
	No (n = 195,773)	Yes (n = 80,486)	P	Never-smokers (n = 175,908)	Adulthood (>18 years) (n = 40,948)	Adolescence (15–18 years) (n = 43,184)	Childhood (5–14 years) (n = 15,804)	P
Major diseases								
Hypertension	104,406 (53.3)	44,137 (54.8)	<0.001	91,809 (52.2)	23,421 (57.2)	25,811 (59.8)	9,368 (59.3)	<0.001
Diabetes	11,082 (5.7)	4,930 (6.1)	<0.001	8,683 (4.9)	2,956 (7.2)	3,312 (7.7)	1,562 (9.9)	<0.001
Cardiovascular diseases	16,970 (8.7)	7,561 (9.4)	<0.001	12,767 (7.3)	4,542 (11.1)	5,388 (12.5)	2,402 (15.2)	<0.001
Cancer	15,284 (7.8)	6,326 (7.9)	0.645	13,019 (7.4)	3,685 (9.0)	3,680 (8.5)	1,223 (7.7)	<0.001
Components of biological aging								
FEV_1 (liters)	2.82 ± 0.81	2.84 ± 0.79	<0.001	2.83 ± 0.81	2.75 ± 0.80	2.79 ± 0.79	2.86 ± 0.80	<0.001
SBP (mmHg)	139.37 ± 19.61	139.39 ± 19.35	0.794	139.19 ± 19.46	140.47 ± 19.78	141.03 ± 19.62	139.34 ± 19.21	<0.001
Total cholesterol (mg/dl)	220.49 ± 43.86	220.82 ± 43.93	0.066	221.28 ± 43.22	221.07 ± 44.85	218.90 ± 45.83	214.99 ± 45.40	<0.001
Glycated hemoglobin (%)	5.44 ± 0.59	5.44 ± 0.60	0.018	5.41 ± 0.57	5.50 ± 0.63	5.51 ± 0.63	5.56 ± 0.72	<0.001
Blood urea nitrogen (mg/dl)	15.08 ± 3.79	15.12 ± 3.88	0.042	15.08 ± 3.70	15.13 ± 4.05	15.22 ± 4.00	15.01 ± 4.25	<0.001
Lymphocyte (%)	29.04 ± 7.46	28.93 ± 7.29	<0.001	29.06 ± 7.42	29.00 ± 7.48	28.66 ± 7.37	28.35 ± 7.32	<0.001
Mean cell volume (fl)	82.78 ± 5.29	82.80 ± 5.32	0.299	82.36 ± 5.15	83.66 ± 5.48	83.41 ± 5.46	83.51 ± 5.67	<0.001
Serum glucose (mg/dl)	91.84 ± 21.15	92.14 ± 22.02	0.001	91.50 ± 20.51	92.81 ± 22.87	92.93 ± 22.87	93.99 ± 26.83	<0.001
Red cell distribution width (%)	13.48 ± 0.97	13.46 ± 0.95	<0.001	13.46 ± 0.97	13.50 ± 0.93	13.50 ± 0.94	13.55 ± 0.99	<0.001
White blood cell count (1000 cells/μl)	6.81 ± 1.92	6.95 ± 1.90	<0.001	6.67 ± 1.81	7.16 ± 1.94	7.28 ± 2.07	7.55 ± 2.25	<0.001
Albumin (g/dl)	45.29 ± 2.60	45.26 ± 2.61	0.002	45.32 ± 2.60	45.17 ± 2.63	45.18 ± 2.61	45.09 ± 2.63	<0.001
Creatinine (mg/dl)	0.81 ± 0.18	0.82 ± 0.18	<0.001	0.81 ± 0.18	0.81 ± 0.19	0.83 ± 0.19	0.85 ± 0.21	<0.001
C-reactive protein (mg/dl)	0.24 ± 0.40	0.27 ± 0.42	<0.001	0.23 ± 0.39	0.27 ± 0.43	0.29 ± 0.44	0.32 ± 0.49	<0.001
Alkaline phosphatase (U/liter)	82.83 ± 25.48	83.46 ± 26.32	<0.001	82.55 ± 25.06	84.26 ± 26.53	85.35 ± 26.79	86.28 ± 27.22	<0.001
Biological aging								
KDM-BA	60.24 ± 8.49	60.14 ± 8.15	0.007	59.45 ± 8.19	62.02 ± 8.29	62.24 ± 8.35	61.19 ± 8.95	<0.001
KDM-BA acceleration	−0.13 ± 3.88	0.21 ± 4.14	<0.001	−0.33 ± 3.71	0.24 ± 4.14	0.75 ± 4.36	1.61 ± 4.84	<0.001
PhenoAge	45.30 ± 10.23	45.23 ± 9.76	0.102	44.29 ± 9.88	47.70 ± 10.06	47.85 ± 9.90	46.83 ± 10.37	<0.001
PhenoAge acceleration	−0.34 ± 5.45	0.08 ± 5.57	<0.001	−0.68 ± 5.30	0.42 ± 5.70	0.91 ± 5.68	2.09 ± 6.06	<0.001
Telomere length	0.84 ± 0.13	0.83 ± 0.13	<0.001	0.84 ± 0.13	0.83 ± 0.13	0.82 ± 0.13	0.82 ± 0.13	<0.001

also revealed that participants who initiated smoking in childhood (5 to 14 years) had the highest acceleration in standardized KDM-BA and PhenoAge, at 0.22 and 0.44, respectively. Considering that each 1-unit increase in standardized accelerated KDM-BA and PhenoAge increased the risk of mortality by 66 and 84% (*31*), respectively, our findings further highlighted the importance of reducing tobacco exposure in early life to improve healthy aging.

The potential mechanisms of accelerated biological aging triggered by early-life tobacco exposure may be involved in oxidative stress, mitochondrial dysfunction, and inflammation (*32*, *33*). Nicotine, polycyclic aromatic hydrocarbons, heavy metals, carbon monoxide, and other poisons contained in tobacco smoke transport the placental barrier and also induce reactive oxygen species (ROS) generation in mononuclear blood cells, inflammation, and endothelial dysfunction, resulting in metabolism alterations (*34*, *35*). Shortened TL, a biomarker of cellular aging, is accelerated because ROS damages telomeric attrition during DNA replication (*36*), which increases the risk of aging-related diseases such as hypertension, cardiovascular and lung events, diabetes, cancer, and dementia (*37*, *38*). In addition to intrauterine exposure, younger age of smoking initiation may

Table 2. Associations of in utero exposure to tobacco smoke and age of smoking initiation with accelerated biological aging. Model 1 was adjusted for age at recruitment and sex.

Early-life tobacco exposure	KDM-BA acceleration (β)		PhenoAge acceleration (β)		Telomere length (percent change)	
	Model 1	Model 2	Model 1	Model 2	Model 1	Model 2
In utero exposure to tobacco smoke*						
No	Reference	Reference	Reference	Reference	Reference	Reference
Yes	0.25 (0.22, 0.28)	0.26 (0.24, 0.29)	0.40 (0.35, 0.44)	0.49 (0.44, 0.53)	−6.09% (−6.84%, −5.34%)	−5.34% (−6.10%, −4.58%)
Age of smoking initiation†						
Never-smokers	Reference	Reference	Reference	Reference	Reference	Reference
Adulthood (>18 years)	0.29 (0.26, 0.33)	0.29 (0.25, 0.33)	1.06 (1.00, 1.11)	1.06 (1.00, 1.12)	−3.96% (−4.96%, −2.94%)	−3.90% (−4.91%, −2.88%)
Adolescence (15–18 years)	0.46 (0.43, 0.50)	0.46 (0.43, 0.50)	1.45 (1.39, 1.50)	1.49 (1.43, 1.54)	−7.54% (−8.49%, −6.58%)	−7.05% (−8.00%, −6.08%)
Childhood (5–14 years)	0.88 (0.83, 0.94)	0.88 (0.83, 0.93)	2.48 (2.39, 2.57)	2.51 (2.42, 2.60)	−11.02% (−12.43%, −9.59%)	−10.53% (−11.95%, −9.10%)
P_{trend}	<0.001	<0.001	<0.001	<0.001	<0.001	<0.001

*Model 2 was adjusted for age at recruitment, sex, ethnicity, and birthplace. †Model 2 was adjusted for age at recruitment, sex, ethnicity, birthplace, and body sizes at age 10 years.

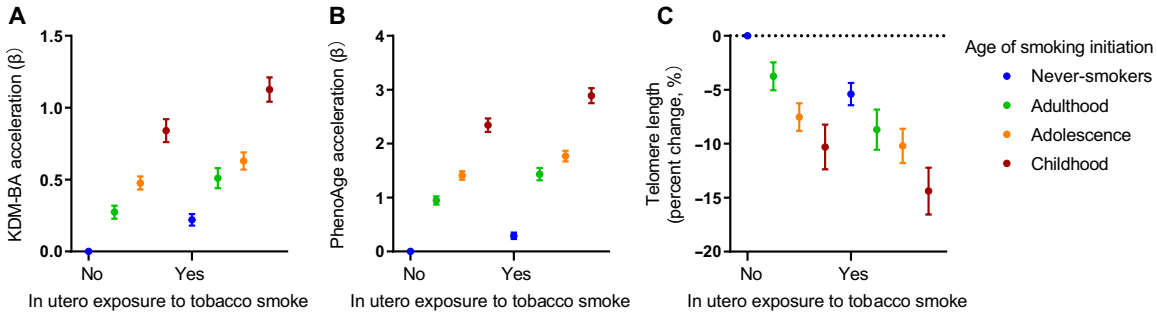

Fig. 1. The joint effects of in utero exposure to tobacco smoke and the age of smoking initiation on accelerated biological aging. (**A**) The β (95% CIs) of KDM-BA acceleration with joint categories of in utero exposure to tobacco smoke and the age of smoking initiation. (**B**) The β (95% CIs) of PhenoAge acceleration with joint categories of in utero exposure to tobacco smoke and the age of smoking initiation. (**C**) The percent change (95% CIs) of telomere length with joint categories of in utero exposure to tobacco smoke and the age of smoking initiation. All models were adjusted for age at recruitment, sex, ethnicity, birthplace, and body sizes at age 10 years.

lead to greater cumulative tobacco exposure (*39*). Smoking in youth may set individuals on a trajectory of increased tobacco use throughout life, greatly increasing their exposure to carcinogens and other toxins and increasing their risk of morbidity and mortality (*20*). Multiple clinical traits of KDM-BA and PhenoAge algorithms are influenced by the above pathways. We also found that the effect of early-life tobacco exposure on PhenoAge acceleration was stronger than that on KDM-BA acceleration. As mentioned in a prior study, aging is a complex biological process, and different BA predictors can capture different biological aging dimensions (*5*). For example, KDM-BA tends to reflect the capacity and function of systems integrity, while PhenoAge is used to predict the mortality risk (*40*, *41*). Furthermore, we observed that high PRS participants with in utero exposure and smoking initiation in childhood had the highest accelerated biological aging, but there was no gene-environment interaction. This result emphasized the important public benefits of early-life tobacco cessation, regardless of genetic background, in resisting biological aging and preventing aging-related diseases.

In this study, the effects of in utero tobacco exposure on accelerated aging were stronger in participants aged ≤50 years than in participants aged ≥61 years. In agreement with our findings, the biological age of young smokers (<40 years) was significantly higher than their CA, but this effect disappeared in the oldest participants (>80 years) (*42*). Another study found that the risk of smoking-related death was extremely high in younger people, while the effect was significantly reduced in older groups (*43*). This could suggest that older smokers who are susceptible as they age may be dying from their habit. Compared to smokers with shorter life spans, surviving smokers may have specific genetic and physiological factors that respond differently to biological stressors, including activation of repair processes and a lower inflammatory response. We also reported that the associations of early-life tobacco exposure with KDM-BA and PhenoAge acceleration were more pronounced among participants who were male and had higher deprivation and unhealthy diet. Similarly, there were significant interactions between early-life tobacco exposure and the TDI on TL. In line with a previous study,

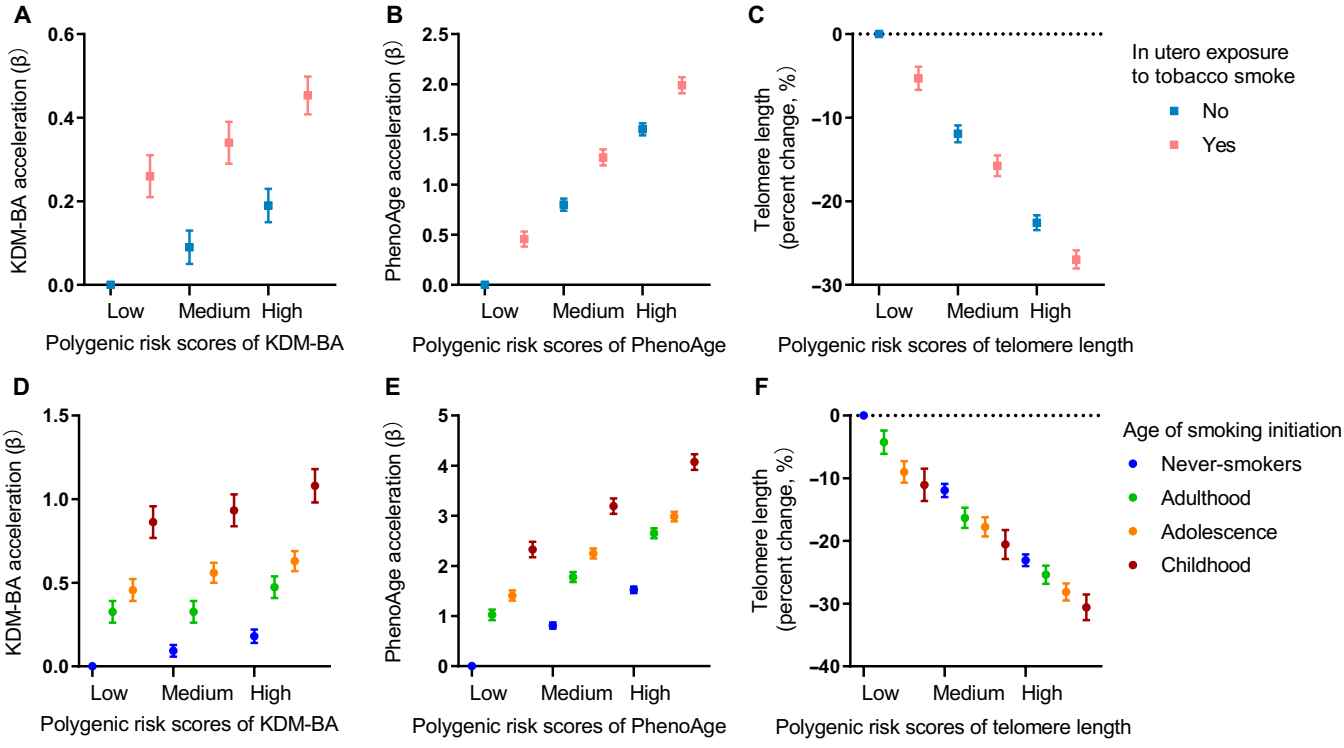

Fig. 2. The joint effects of in utero exposure to tobacco smoke or the age of smoking initiation and genetic susceptibility on accelerated biological aging. (**A**) The β (95% CIs) of KDM-BA acceleration with joint categories of in utero exposure to tobacco smoke and PRS of KDM-BA. (**B**) The β (95% CIs) of PhenoAge acceleration with joint categories of in utero exposure to tobacco smoke and polygenic risk scores of PhenoAge. (**C**) The percent change (95% CIs) of telomere length with joint categories of in utero exposure to tobacco smoke and polygenic risk scores of telomere length. (**D**) The β (95% CIs) of KDM-BA acceleration with joint categories of the age of smoking initiation and polygenic risk scores of KDM-BA. (**E**) The β (95% CIs) of PhenoAge acceleration with joint categories of the age of smoking initiation and polygenic risk scores of PhenoAge. (**F**) The percent change (95% CIs) of telomere length with joint categories of the age of smoking initiation and polygenic risk scores of telomere length. (A) to (C) Models were adjusted for age at recruitment, sex, ethnicity, birthplace, genotyping batch, and the first 10 genetic principal components. (D) to (F) Models were adjusted for age at recruitment, sex, ethnicity, birthplace, body sizes at age 10 years, genotyping batch, and the first 10 genetic principal components.

tobacco use, unhealthy diet, and increased pressure such as income, housing, and economic independence were related to increases in epigenetic aging among middle-aged Black women (*44*). Childhood poverty was a potential precipitant of epigenetic age acceleration in 490 midlife and older people (*45*). The discrepancy in other interactions between demographic characteristics and early-life tobacco exposure on three indicators of biological aging may be due to different aspects of biological aging explained by indicators. Further research is needed to validate these findings.

The strengths of our study included comprehensive BA estimation in a large-scale biobank cohort to improve the accuracy of BA predictions, temporality from early-life tobacco exposure to the outcome, and directed acyclic graphs (DAGs) to identify potential confounders. Nevertheless, some limitations of the present study should be acknowledged. First, we did not obtain detailed information on the duration and pack-years of smoking, environmental tobacco, and secondhand smoke in the early-life stages. Second, data on early-life tobacco exposure were retrospectively collected by self-reported questionnaires, leading to recall bias. However, previous literature has depicted that the offspring's report of in utero tobacco exposure was a good proxy measure for the mother's own report of smoking during pregnancy (*46*). The prevalence of smoking during pregnancy was similar between this study (29.1%) and a study carried out in the United Kingdom (23.3%) (*30*). Moreover, results were highly consistent across repeated assessments of the same perinatal maternal smoking between baseline, first, and second surveys (kappa > 0.90). Given the social undesirability bias, tobacco exposure is commonly underreported (*47*). Nondifferential misclassification would attenuate any true causal association. However, we still observed significant associations of early-life tobacco exposure with accelerated biological aging. To provide accuracy in tobacco exposure, repeated measurements of nicotine and its metabolites in various biological specimens are needed in the future. Third, we only estimated BA and TL at baseline and could not explore the effect of early-life tobacco exposure on the rates of biological aging changes over time. Fourth, residual and unmeasured confounders in early-life stages, such as parental characteristics and maternal weight during pregnancy, may mix the estimated effects. However, the DAG method can partially avoid the effects of missing and unmeasured confounders. We also conducted a series of sensitivity analyses to confirm the validity of our findings, such as adjusting for potential adult covariates and mediators, in which all results were robust. Additionally, our study with a cross-sectional nature cannot interpret the causal association between early-life tobacco exposure and biological aging. Lastly, participants from the UK Biobank were healthier and about 94% white and had higher socioeconomic status, which should be cautiously extrapolated. More prospective cohorts of other ethnic populations are needed to validate our findings.

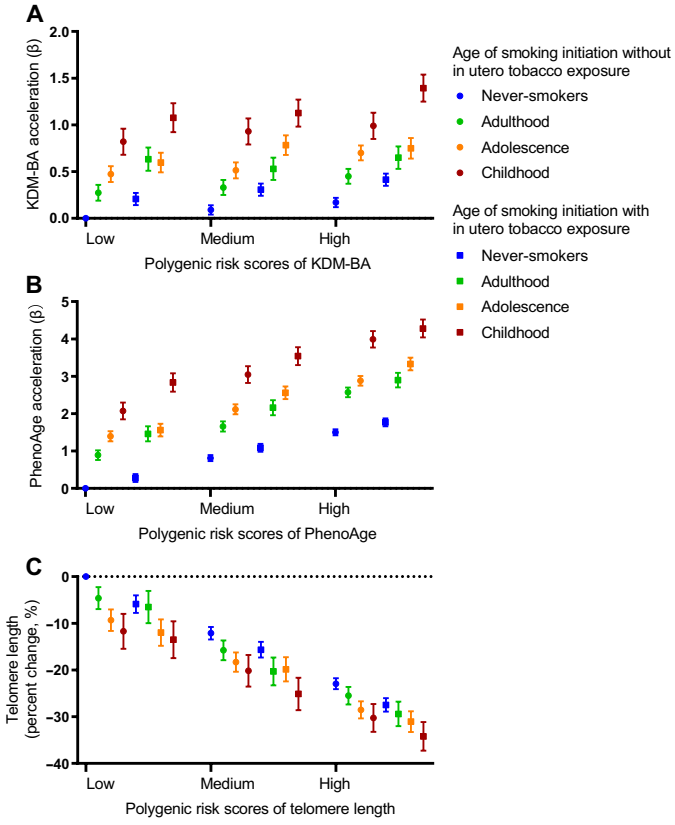

Fig. 3. The joint effects of in utero exposure to tobacco smoke, the age of smoking initiation, and genetic susceptibility on accelerated biological aging. (**A**) The β (95% CIs) of KDM-BA acceleration with joint categories of in utero exposure to tobacco smoke, the age of smoking initiation, and polygenic risk scores of KDM-BA. (**B**) The β (95% CIs) of PhenoAge acceleration with joint categories of in utero exposure to tobacco smoke, the age of smoking initiation, and polygenic risk scores of PhenoAge. (**C**) The percent change (95% CIs) of telomere length with joint categories of in utero exposure to tobacco smoke, the age of smoking initiation, and polygenic risk scores of telomere length. Models were adjusted for age at recruitment, sex, ethnicity, birthplace, body sizes at age 10 years, genotyping batch, and the first 10 genetic principal components.

In summary, we provided evidence based on a large-scale epidemiological survey that exposure to tobacco in the fetal period, childhood, adolescence, and adulthood was significantly associated with accelerated BA and shortened TL later in life independent of genetic susceptibility. Furthermore, high PRS individuals with in utero exposure and smoking initiation in childhood had the highest accelerated biological aging. The present study highlighted the important role of reducing tobacco exposure from the fetal period throughout childhood, adolescence, and adulthood to promote longevity and prevent aging-related diseases. Further studies are warranted to elucidate the underlying mechanisms.

METHODS

Study design and population

The data in our study were derived from the UK Biobank, which was an ongoing population-based cohort study with approximately 0.5 million participants (aged 37 to 73 years) enrolled in 2006 to 2010, as detailed previously (*48*). The study protocols received approval from the National Information Governance Board for Health and Social Care and the National Health Service North West Multicenter Research Ethics Committee. All participants signed an electronic informed consent at baseline assessment. This analysis was from application number 69741. Figure S2 shows the datasets constructed. After the exclusions of participants without information on biological aging and early-life tobacco exposure, a total of 276,259 (275,844) participants were used to examine the association between in utero tobacco exposure (age of smoking initiation) and accelerated biological aging. Furthermore, we performed quality control on genetic data to explore the joint effects of early-life tobacco exposure and genetic susceptibility on accelerated biological aging among participants of European descent.

Assessment of early-life tobacco exposure

Early-life tobacco exposure was assessed by self-reported questionnaires, including exposure to tobacco in utero and the age of smoking initiation (*12*, *14*). Exposure to tobacco in utero was collected by this item: "Did your mother smoke regularly around the time when you were born?" Maternal smoking around birth (Data-Field 1787) was collected except for those who indicated they were adopted as a child (Data-Field 1767). Age of smoking initiation was defined through the following items: smoking status (Data-Field 20116), age started smoking in current smokers (Data-Field 3436), and age started smoking in former smokers (Data-Field 2867). Then, participants were divided into four groups based on the age of smoking initiation: never-smokers, adulthood (>18 years), adolescence (15 to 18 years), and childhood (5 to 14 years).

Assessment of biological age and age acceleration

BA, including KDM-BA and PhenoAge, has been measured by the best-trained algorithms from the National Health and Nutrition Examination Survey (NHANES) (*41*, *49*, *50*), which has also been validated using available data on anthropometric measurements and biochemical markers from the UK Biobank (*23*, *51*). The blood specimens collected at baseline were analyzed with the Beckman Coulter LH750 instruments within 24 hours. Detailed processes and quality control of biomarkers were obtained on the website (https://biobank.ndph.ox.ac.uk/showcase/showcase/docs/serum_biochemistry.pdf). Table S10 lists the corresponding data-field IDs of biomarkers for the construction of BA. The BioAge R package was used to calculate values of KDM-BA and PhenoAge (http://github.com/dayoonkwon/BioAge), where missing data of components of BA were excluded. In the package, the reference population with complete biomarker data includes 7694 nonpregnant participants (aged 30 to 75 years) for KDM-BA and 12,998 participants (aged 20 to 84 years) for PhenoAge in the NHANES III (*52*).

KDM-BA was derived from regressions of nine biomarkers [e.g., systolic blood pressure, forced expiratory volume in 1 s (FEV_1), total cholesterol, glycated hemoglobin, blood urea nitrogen, albumin, creatinine, C-reactive protein, and alkaline phosphatase] on CA in a reference population, approximately corresponding to physiologically normal CA.The equation is

$$\mathrm{KDM-BA} = \frac{\sum_{i=1}^{n}(x_i - q_i)\frac{k_i}{s_i^2} + \frac{\mathrm{CA}}{s_{\mathrm{BA}}^2}}{\sum_{i=1}^{n}\left(\frac{k_i}{s_i}\right)^2 + \frac{1}{s_{\mathrm{BA}}^2}}$$

where x_i is the value of each biomarker for an individual; k_i, q_i, and s_i are the intercept, slope, and root mean square error, respectively, which were estimated from the regression of CA on each biomarker separately for men and women; s_{BA} is the square root of the variance in CA explained by the biomarker set; and $n = 9$, namely, the total number of biomarkers in this study.

PhenoAge was interpreted as the age at which the average mortality risk matches the predicted mortality risk, and its algorithm was constructed using elastic-net Gompertz regression of mortality risk on 42 biomarkers among NHANES III participants, resulting in nine biomarkers and CA selected as a parsimonious model to calculate the mortality prediction score. In our study, we computed an individual's PhenoAge through CA and nine biomarkers, including lymphocyte percentage, mean sphered cell volume, glucose, red cell distribution width, white blood cell count, albumin, creatinine, C-reactive protein, and alkaline phosphatase. The formula is as follows

$$\text{PhenoAge} = 141.50225 + \frac{\ln[-0.00553 \times \ln(1-\text{mortality risk})]}{0.090165}$$

$$\text{where mortality risk} = 1 - e^{-e^{xb}[\exp(120\times\gamma)-1]/\gamma},\ \gamma = 0.0076927,$$

$$xb = -19.907 + 0.0804 \times \text{CA} - 0.012 \times \text{lymphocyte percentage} +$$
$$0.0268 \times \text{mean sphered cell volume} + 0.1953 \times \text{glucose} +$$
$$0.3306 \times \text{red cell distribution width} +$$
$$0.0554 \times \text{white blood cell count} - 0.0336 \times \text{albumin} +$$
$$0.0095 \times \text{creatinine} +$$
$$0.0954 \times \ln(\text{C} - \text{reactive protein}) +$$
$$0.00188 \times \text{alkaline phosphatase}$$

To quantify the deviation between BA and CA, the residuals were computed using linear regressions of KDM-BA and PhenoAge on their CA, called age acceleration (*51*). Individuals with age acceleration values greater than 0 indicated an advanced state of biological aging, and vice versa (*52*).

Measurements of leukocyte TL

TL in peripheral blood leukocytes was determined using the multiplex quantitative polymerase chain reaction technique by researchers at the University of Leicester in England (*53*). TL was a ratio of TL repeat number (T) against a reference single-copy gene (S) to express a T/S ratio, where T and S were computed by either the calibrator sample at each run consisting of pooled DNA from 20 participants or the standard curve. Considering skewed distribution and the difference in T/S ratios due to different quantification methods, the natural logarithm-transformed z-standardized T/S ratio (Data-Field 22192) was conducted using the distribution of all individuals with a TL measurement, which was used in this study.

Polygenic risk scores

PRS was constructed according to genetic variants associated with aging phenotypes and leukocyte TL in European-descent participants from the previously published genome-wide association studies (*22*, *23*). Table S11 summarizes the single-nucleotide polymorphisms (SNPs) ($P < 5 \times 10^{-8}$ and minor allele frequency > 0.05) used for constructing PRS of PhenoAge, KDM-BA, and TL. Detailed information regarding SNP genotyping, imputation, and quality control in the UK Biobank was described previously (*54*). The formula for PRS calculation is as follows:

$$\text{PRS} = \sum_{i=1}^{m} \beta_i \times \text{SNP}_i$$

where β_i is the per-allele effect from genome-wide association study; SNP_i is the number of effect alleles, and m is the total number of SNPs associated with PhenoAge, KDM-BA, and TL (29, 15, and 18, respectively). These PRS were categorized into low (lowest tertile), medium (tertile 2), and high (highest tertile) risk.

Covariates

On the basis of prior literature and DAG (*55*) (fig. S3), models were adjusted for potential confounders. The covariates included demographic characteristics (e.g., age at recruitment, sex, BMI, ethnicity, TDI, birthplace, and the body and height sizes at age 10 years), lifestyles (e.g., drinking status, physical activity, healthy diet score, and air pollution), and major diseases at recruitment (e.g., hypertension, diabetes, CVDs, and cancer). The detailed codes of major diseases at recruitment are presented in table S12. The TDI was assessed on four dimensions: unemployment, non-car ownership, overcrowded household, and non-home ownership. Higher levels of the TDI indicated higher levels of deprivation. Physical activity was estimated by the sum of metabolic equivalent task (MET) minutes per week according to the International Physical Activity Questionnaire. The healthy diet score was computed using the frequency of intake of common food, including fresh fruit, vegetables, fish, processed meat, and unprocessed red meat (table S13) (*56*). Annual average air pollution levels of individuals were quantified using the land use regression models (Supplementary Text 1) (*57*, *58*). In addition, because of the high missing data on birth weight (44.9%) and its colinearity with the body shape, the models were adjusted for available body sizes at age 10 years.

Statistical analysis

We performed all analyses by using R version 4.2.2 (R Foundation for Statistical Computing). All *P* values were obtained by two-sided tests with statistical significance set at <0.05. The characteristics of the analytic participants were presented across in utero exposure to tobacco smoke and the age of smoking initiation as counts (percentage) for categorical variables and means ± SDs for continuous variables. Missing values for categorical variables were encoded as a missing indicator category, and missing data for continuous variables were replaced with the median value. We also calculated the Pearson correlation coefficients of CA, KDM-BA, PhenoAge, and age acceleration.

The analytic plane of this study is listed in fig. S2. We conducted multivariate general linear regression models to estimate the associations of early-life tobacco exposure and PRS with KDM-BA and PhenoAge acceleration and documented regression coefficient (β) and corresponding 95% CIs. Linear regression models were used to examine the effects of early-life tobacco exposure and PRS on TL. The percent changes were expressed using the following formula: $[\exp(\beta) - 1] \times 100\%$. Model 1 was adjusted for age at recruitment and sex. Model 2 was further adjusted for ethnicity and birthplace for in utero exposure to tobacco smoke and further adjusted for ethnicity, birthplace, and body sizes at age 10 years for the age of smoking initiation. Furthermore, we adjusted for the genotyping batch and the first 10 genetic principal components in the analyses

of PRS. The linear trend across the age of smoking initiation was tested using the integer values.

When analyzing the combined effects of in utero exposure to tobacco smoke and the age of smoking initiation, we classified the participants into eight subgroups and set unexposed to tobacco in utero and never-smokers as the reference group (analysis 2). Moreover, to examine whether the genetic susceptibility to BA may modify the association of early-life tobacco exposure with accelerated biological aging, we set cross-product terms in the model and additionally explore the joint association of early-life tobacco exposure and PRS (analysis 3). We also categorized the participants into 24 groups based on early-life tobacco exposure, age of smoking initiation, and PRS to analyze their joint effects on biological aging, with a reference group of individuals at low genetic risk, unexposed to tobacco in utero, and never-smokers (analysis 4).

In addition, we also conducted a series of stratified analyses to evaluate potential modification effects by the following characteristics: age at recruitment (≤50, 51 to 60, or ≥61), sex (female versus male), TDI (<median versus ≥median), and healthy diet score (0 to 1, 2 to 3, or 4 to 5). The potential modification effects were evaluated by fitting the cross-product term of the stratifying characteristics with early-life tobacco exposure.

Several sensitivity analyses were conducted to evaluate the robustness of the results. First, we restricted the analyses among participants with complete covariates and European descent. Furthermore, to allow comparison of the effect sizes, the residuals of KDM-BA and PhenoAge were standardized with a mean (0) and SD (1) (*51*). Third, we additionally adjusted for BMI, TDI, physical activity, drinking status, healthy diet score, air pollution, body and height sizes at age 10 years, and major diseases in model 3 to address potential residual confounding. Because of the relatively strong correlation between air pollutants (*56*), model 3 was adjusted for a single air pollutant (NO_2, NO_x, $PM_{2.5}$, or PM_{10}). Last, to avoid inappropriate estimation of the residual scale from linear regression, robust linear regression models were used to assess the association between exposure and outcome (*59*).

Supplementary Materials

This PDF file includes:

Supplementary Texts 1 and 2
Tables S1 to S13
Figs. S1 to S3

REFERENCES AND NOTES

1. L. Ferrucci, M. E. Levine, P. L. Kuo, E. M. Simonsick, Time and the metrics of aging. *Circ. Res.* **123**, 740–744 (2018).
2. B. K. Kennedy, S. L. Berger, A. Brunet, J. Campisi, A. M. Cuervo, E. S. Epel, C. Franceschi, G. J. Lithgow, R. I. Morimoto, J. E. Pessin, T. A. Rando, A. Richardson, E. E. Schadt, T. Wyss-Coray, F. Sierra, Geroscience: Linking aging to chronic disease. *Cell* **159**, 709–713 (2014).
3. V. Atella, A. Piano Mortari, J. Kopinska, F. Belotti, F. Lapi, C. Cricelli, L. Fontana, Trends in age-related disease burden and healthcare utilization. *Aging Cell* **18**, e12861 (2019).
4. J. Jylhava, N. L. Pedersen, S. Hagg, Biological age predictors. *EBioMedicine* **21**, 29–36 (2017).
5. H. Bao, J. Cao, M. Chen, M. Chen, W. Chen, X. Chen, Y. Chen, Y. Chen, Y. Chen, Z. Chen, J. K. Chhetri, Y. Ding, J. Feng, J. Guo, M. Guo, C. He, Y. Jia, H. Jiang, Y. Jing, D. Li, J. Li, J. Li, Q. Liang, R. Liang, F. Liu, X. Liu, Z. Liu, O. J. Luo, J. Lv, J. Ma, K. Mao, J. Nie, X. Qiao, X. Sun, X. Tang, J. Wang, Q. Wang, S. Wang, X. Wang, Y. Wang, Y. Wang, R. Wu, K. Xia, F. H. Xiao, L. Xu, Y. Xu, H. Yan, L. Yang, R. Yang, Y. Yang, Y. Ying, L. Zhang, W. Zhang, W. Zhang, X. Zhang, Z. Zhang, M. Zhou, R. Zhou, Q. Zhu, Z. Zhu, F. Cao, Z. Cao, P. Chan, C. Chen, G. Chen, H. Z. Chen, J. Chen, W. Ci, B. S. Ding, Q. Ding, F. Gao, J. J. Han, K. Huang, Z. Ju, Q. P. Kong, J. Li, J. Li, X. Li, B. Liu, F. Liu, L. Liu, Q. Liu, Q. Liu, X. Liu, Y. Liu, X. Luo, S. Ma, X. Ma, Z. Mao, J. Nie, Y. Peng, J. Qu, J. Ren, R. Ren, M. Song, Z. Songyang, Y. E. Sun, Y. Sun, M. Tian, S. Wang, S. Wang, X. Wang, X. Wang, Y. J. Wang, Y. Wang, C. C. L. Wong, A. P. Xiang, Y. Xiao, Z. Xie, D. Xu, J. Ye, R. Yue, C. Zhang, H. Zhang, L. Zhang, W. Zhang, Y. Zhang, Y. W. Zhang, Z. Zhang, T. Zhao, Y. Zhao, D. Zhu, W. Zou, G. Pei, G. H. Liu, Biomarkers of aging. *Sci. China Life Sci.* **66**, 893–1066 (2023).
6. D. W. Belsky, T. E. Moffitt, A. A. Cohen, D. L. Corcoran, M. E. Levine, J. A. Prinz, J. Schaefer, K. Sugden, B. Williams, R. Poulton, A. Caspi, Eleven telomere, epigenetic clock, and biomarker-composite quantifications of biological aging: Do they measure the same thing? *Am. J. Epidemiol.* **187**, 1220–1230 (2018).
7. X. Li, A. Ploner, Y. Wang, P. K. Magnusson, C. Reynolds, D. Finkel, N. L. Pedersen, J. Jylhävä, S. Hägg, Longitudinal trajectories, correlations and mortality associations of nine biological ages across 20-years follow-up. *eLife* **9**, e51507 (2020).
8. D. J. Lowsky, S. J. Olshansky, J. Bhattacharya, D. P. Goldman, Heterogeneity in healthy aging. *J. Gerontol. A Biol. Sci. Med. Sci.* **69**, 640–649 (2014).
9. M. W. Gillman, Developmental origins of health and disease. *N. Engl. J. Med.* **353**, 1848–1850 (2005).
10. R. Barouki, P. D. Gluckman, P. Grandjean, M. Hanson, J. J. Heindel, Developmental origins of non-communicable disease: Implications for research and public health. *Environ. Health* **11**, 42 (2012).
11. D. S. Bui, C. J. Lodge, J. A. Burgess, A. J. Lowe, J. Perret, M. Q. Bui, G. Bowatte, L. Gurrin, D. P. Johns, B. R. Thompson, G. S. Hamilton, P. A. Frith, A. L. James, P. S. Thomas, D. Jarvis, C. Svanes, M. Russell, S. C. Morrison, I. Feather, K. J. Allen, R. Wood-Baker, J. Hopper, G. G. Giles, M. J. Abramson, E. H. Walters, M. C. Matheson, S. C. Dharmage, Childhood predictors of lung function trajectories and future COPD risk: A prospective cohort study from the first to the sixth decade of life. *Lancet Respir. Med.* **6**, 535–544 (2018).
12. Z. Ye, J. Li, P. Gu, Y. Zhang, Y. Xie, S. Yang, Y. Yao, X. You, M. Xue, J. Ma, Early-life tobacco smoke exposure, genetic susceptibility and the risk of type 2 diabetes in adulthood: A large prospective cohort study. *Sci. Total Environ.* **893**, 164698 (2023).
13. D. R. Jacobs Jr., J. G. Woo, A. R. Sinaiko, S. R. Daniels, J. Ikonen, M. Juonala, N. Kartiosuo, T. Lehtimäki, C. G. Magnussen, J. S. A. Viikari, N. Zhang, L. A. Bazzano, T. L. Burns, R. J. Prineas, J. Steinberger, E. M. Urbina, A. J. Venn, O. T. Raitakari, T. Dwyer, Childhood cardiovascular risk factors and adult cardiovascular events. *N. Engl. J. Med.* **386**, 1877–1888 (2022).
14. H. He, M. M. He, H. Wang, W. Qiu, L. Liu, L. Long, Q. Shen, S. Zhang, S. Qin, Z. Lu, Y. Cai, M. Zhang, S. Niu, J. Li, N. Shen, Y. Zhu, J. Tian, J. Chang, X. Miao, R. Zhong, In utero and childhood/adolescence exposure to tobacco smoke, genetic risk, and lung cancer incidence and mortality in adulthood. *Am. J. Respir. Crit. Care Med.* **207**, 173–182 (2023).
15. B. Thomson, N. A. Rojas, B. Lacey, J. A. Burrett, P. Varona-Pérez, M. C. Martínez, E. Lorenzo-Vázquez, S. B. Constantén, J. M. Morales Rigau, O. J. Hernández López, M. Martínez Morales, I. A. Alomá, F. A. Estupiñan, M. D. González, N. R. Muñoz, M. C. Asencio, J. Emberson, R. Peto, S. Lewington, A. D. Herrera, Association of childhood smoking and adult mortality: Prospective study of 120 000 Cuban adults. *Lancet Glob. Health* **8**, e850–e857 (2020).
16. H. M. Salihu, A. Pradhan, L. King, A. Paothong, C. Nwoga, P. J. Marty, V. Whiteman, Impact of intrauterine tobacco exposure on fetal telomere length. *Am. J. Obstet. Gynecol.* **212**, e201–e208 (2015).
17. P. Ip, B. H. Chung, F. K. Ho, G. C. Chan, W. Deng, W. H. Wong, S. L. Lee, P. Y. Chan, D. Ying, W. L. Wong, K. T. Tung, Y. L. Lau, Prenatal tobacco exposure shortens telomere length in children. *Nicotine Tob. Res.* **19**, 111–118 (2017).
18. C. Osorio-Yanez, D. B. P. Clemente, L. Maitre, M. Vives-Usano, M. Bustamante, D. Martinez, M. Casas, J. Alexander, C. Thomsen, L. Chatzi, K. B. Gutzkow, R. Grazuleviciene, D. S. Martens, M. Plusquin, R. Slama, R. C. McEachan, J. Wright, T. C. Yang, J. Urquiza, I. Tamayo, J. Sunyer, M. Vafeiadi, T. S. Nawrot, M. Vrijheid, Early life tobacco exposure and children's telomere length: The HELIX project. *Sci. Total Environ.* **711**, 135028 (2020).
19. P. de Prado-Bert, C. Ruiz-Arenas, M. Vives-Usano, S. Andrusaityte, S. Cadiou, A. Carracedo, M. Casas, L. Chatzi, P. Dadvand, J. R. Gonzalez, R. Grazuleviciene, K. B. Gutzkow, L. S. Haug, C. Hernandez-Ferrer, H. C. Keun, J. Lepeule, L. Maitre, R. McEachan, M. J. Nieuwenhuijsen, D. Pelegri, O. Robinson, R. Slama, M. Vafeiadi, J. Sunyer, M. Vrijheid, M. Bustamante, The early-life exposome and epigenetic age acceleration in children. *Environ. Int.* **155**, 106683 (2021).
20. E. T. Klopack, J. E. Carroll, S. W. Cole, T. E. Seeman, E. M. Crimmins, Lifetime exposure to smoking, epigenetic aging, and morbidity and mortality in older adults. *Clin. Epigenetics* **14**, 72 (2022).
21. S. S. Khan, B. D. Singer, D. E. Vaughan, Molecular and physiological manifestations and measurement of aging in humans. *Aging Cell* **16**, 624–633 (2017).
22. C. Li, S. Stoma, L. A. Lotta, S. Warner, E. Albrecht, A. Allione, P. P. Arp, L. Broer, J. L. Buxton, A. D. S. C. Alves, J. Deelen, I. O. Fedko, S. D. Gordon, T. Jiang, R. Karlsson, N. Kerrison, T. K. Loe, M. Mangino, Y. Milaneschi, B. Miraglio, N. Pervjakova, A. Russo, I. Surakka, A. van der Spek, J. E. Verhoeven, N. Amin, M. Beekman, A. I. Blakemore, F. Canzian, S. E. Hamby, J. J. Hottenga, P. D. Jones, P. Jousilahti, R. Magi, S. E. Medland, G. W. Montgomery, D. R. Nyholt, M. Perola, K. H. Pietilainen, V. Salomaa, E. Sillanpaa, H. E. Suchiman, D. van Heemst, G. Willemsen, A. Agudo, H. Boeing, D. I. Boomsma,

M. D. Chirlaque, G. Fagherazzi, P. Ferrari, P. Franks, C. Gieger, J. G. Eriksson, M. Gunter, S. Hagg, I. Hovatta, L. Imaz, J. Kaprio, R. Kaaks, T. Key, V. Krogh, N. G. Martin, O. Melander, A. Metspalu, C. Moreno, N. C. Onland-Moret, P. Nilsson, K. K. Ong, K. Overvad, D. Palli, S. Panico, N. L. Pedersen, B. Penninx, J. R. Quiros, M. R. Jarvelin, M. Rodriguez-Barranco, R. A. Scott, G. Severi, P. E. Slagboom, T. D. Spector, A. Tjonneland, A. Trichopoulou, R. Tumino, A. G. Uitterlinden, Y. T. van der Schouw, C. M. van Duijn, E. Weiderpass, E. L. Denchi, G. Matullo, A. S. Butterworth, J. Danesh, N. J. Samani, N. J. Wareham, C. P. Nelson, C. Langenberg, V. Codd, Genome-wide association analysis in humans links nucleotide metabolism to leukocyte telomere length. *Am. J. Hum. Genet.* **106**, 389–404 (2020).

23. C. L. Kuo, L. C. Pilling, Z. Liu, J. L. Atkins, M. E. Levine, Genetic associations for two biological age measures point to distinct aging phenotypes. *Aging Cell* **20**, e13376 (2021).
24. X. Gao, N. Huang, X. Guo, T. Huang, Role of sleep quality in the acceleration of biological aging and its potential for preventive interaction on air pollution insults: Findings from the UK Biobank cohort. *Aging Cell* **21**, e13610 (2022).
25. J. Zhu, Y. Yang, Y. Zeng, X. Han, W. Chen, Y. Hu, Y. Qu, H. Yang, U. A. Valdimarsdóttir, F. Fang, H. Song, The association of physical activity behaviors and patterns with aging acceleration: Evidence from the UK Biobank. *J. Gerontol. A Biol. Sci. Med. Sci.* **78**, 753–761 (2023).
26. A. Vriens, T. S. Nawrot, B. G. Janssen, W. Baeyens, L. Bruckers, A. Covaci, S. De Craemer, S. De Henauw, E. Den Hond, I. Loots, V. Nelen, T. Schettgen, G. Schoeters, D. S. Martens, M. Plusquin, Exposure to environmental pollutants and their association with biomarkers of aging: A multipollutant approach. *Environ. Sci. Technol.* **53**, 5966–5976 (2019).
27. R. O. Wright, Environment, susceptibility windows, development, and child health. *Curr. Opin. Pediatr.* **29**, 211–217 (2017).
28. J. Clark, C. M. Bulka, C. L. Martin, K. Roell, H. P. Santos, T. M. O'Shea, L. Smeester, R. Fry, R. Dhingra, Placental epigenetic gestational aging in relation to maternal sociodemographic factors and smoking among infants born extremely preterm: A descriptive study. *Epigenetics* **17**, 2389–2403 (2022).
29. A. K. Bozack, S. L. Rifas-Shiman, D. R. Gold, Z. M. Laubach, W. Perng, M. F. Hivert, A. Cardenas, DNA methylation age at birth and childhood: Performance of epigenetic clocks and characteristics associated with epigenetic age acceleration in the Project Viva cohort. *Clin. Epigenetics* **15**, 62 (2023).
30. S. Lange, C. Probst, J. Rehm, S. Popova, National, regional, and global prevalence of smoking during pregnancy in the general population: A systematic review and meta-analysis. *Lancet Glob. Health* **6**, e769–e776 (2018).
31. J. K. L. Mak, C. E. McMurran, R. Kuja-Halkola, P. Hall, K. Czene, J. Jylhävä, S. Hägg, Clinical biomarker-based biological aging and risk of cancer in the UK Biobank. *Br. J. Cancer* **129**, 94–103 (2023).
32. M. A. Babizhayev, Y. E. Yegorov, Smoking and health: Association between telomere length and factors impacting on human disease, quality of life and life span in a large population-based cohort under the effect of smoking duration. *Fundam. Clin. Pharmacol.* **25**, 425–442 (2011).
33. J. Huang, M. Okuka, M. McLean, D. L. Keefe, L. Liu, Effects of cigarette smoke on fertilization and embryo development in vivo. *Fertil. Steril.* **92**, 1456–1465 (2009).
34. G. Banderali, A. Martelli, M. Landi, F. Moretti, F. Betti, G. Radaelli, C. Lassandro, E. Verduci, Short and long term health effects of parental tobacco smoking during pregnancy and lactation: A descriptive review. *J. Transl. Med.* **13**, 327 (2015).
35. A. Rua Ede, M. L. Porto, J. P. Ramos, B. V. Nogueira, S. S. Meyrelles, E. C. Vasquez, T. C. Pereira, Effects of tobacco smoking during pregnancy on oxidative stress in the umbilical cord and mononuclear blood cells of neonates. *J. Biomed. Sci.* **21**, 105 (2014).
36. J. M. Houben, H. J. Moonen, F. J. van Schooten, G. J. Hageman, Telomere length assessment: Biomarker of chronic oxidative stress? *Free Radic. Biol. Med.* **44**, 235–246 (2008).
37. C. V. Schneider, K. M. Schneider, A. Teumer, K. L. Rudolph, D. Hartmann, D. J. Rader, P. Strnad, Association of telomere length with risk of disease and mortality. *JAMA Intern. Med.* **182**, 291–300 (2022).
38. V. Codd, Q. Wang, E. Allara, C. Musicha, S. Kaptoge, S. Stoma, T. Jiang, S. E. Hamby, P. S. Braund, V. Bountziouka, C. A. Budgeon, M. Denniff, C. Swinfield, M. Papakonstantinou, S. Sheth, D. E. Nanus, S. C. Warner, M. Wang, A. V. Khera, J. Eales, W. H. Ouwehand, J. R. Thompson, E. Di Angelantonio, A. M. Wood, A. S. Butterworth, J. N. Danesh, C. P. Nelson, N. J. Samani, Polygenic basis and biomedical consequences of telomere length variation. *Nat. Genet.* **53**, 1425–1433 (2021).
39. J. K. Wiencke, K. T. Kelsey, Teen smoking, field cancerization, and a "critical period" hypothesis for lung cancer susceptibility. *Environ. Health Perspect.* **110**, 555–558 (2002).
40. S. Hägg, D. W. Belsky, A. A. Cohen, Developments in molecular epidemiology of aging. *Emerg. Top Life Sci.* **3**, 411–421 (2019).
41. Z. Liu, P. L. Kuo, S. Horvath, E. Crimmins, L. Ferrucci, M. Levine, A new aging measure captures morbidity and mortality risk across diverse subpopulations from NHANES IV: A cohort study. *PLoS Med.* **15**, e1002718 (2018).
42. P. Mamoshina, K. Kochetov, F. Cortese, A. Kovalchuk, A. Aliper, E. Putin, M. Scheibye-Knudsen, C. R. Cantor, N. M. Skjodt, O. Kovalchuk, A. Zhavoronkov, Blood biochemistry analysis to detect smoking status and quantify accelerated aging in smokers. *Sci. Rep.* **9**, 142 (2019).
43. M. Levine, E. Crimmins, Not all smokers die young: A model for hidden heterogeneity within the human population. *PLOS ONE* **9**, e87403 (2014).
44. R. L. Simons, M. L. Ong, M. K. Lei, E. Klopack, M. Berg, Y. Zhang, R. Philibert, F. X. Gibbons, S. R. H. Beach, Shifts in lifestyle and socioeconomic circumstances predict change-for better or worse-in speed of epigenetic aging: A study of middle-aged black women. *Soc. Sci. Med.* **307**, 115175 (2022).
45. C. McCrory, G. Fiorito, A. M. O'Halloran, S. Polidoro, P. Vineis, R. A. Kenny, Early life adversity and age acceleration at mid-life and older ages indexed using the next-generation GrimAge and Pace of Aging epigenetic clocks. *Psychoneuroendocrinology* **137**, 105643 (2022).
46. J. F. Simard, B. A. Rosner, K. B. Michels, Exposure to cigarette smoke in utero: Comparison of reports from mother and daughter. *Epidemiology* **19**, 628–633 (2008).
47. S. S. Coughlin, Recall bias in epidemiologic studies. *J. Clin. Epidemiol.* **43**, 87–91 (1990).
48. C. Sudlow, J. Gallacher, N. Allen, V. Beral, P. Burton, J. Danesh, P. Downey, P. Elliott, J. Green, M. Landray, B. Liu, P. Matthews, G. Ong, J. Pell, A. Silman, A. Young, T. Sprosen, T. Peakman, R. Collins, UK Biobank: An open access resource for identifying the causes of a wide range of complex diseases of middle and old age. *PLoS Med.* **12**, e1001779 (2015).
49. P. Klemera, S. Doubal, A new approach to the concept and computation of biological age. *Mech. Ageing Dev.* **127**, 240–248 (2006).
50. M. E. Levine, Modeling the rate of senescence: Can estimated biological age predict mortality more accurately than chronological age? *J. Gerontol. A Biol. Sci. Med. Sci.* **68**, 667–674 (2013).
51. X. Gao, T. Geng, M. Jiang, N. Huang, Y. Zheng, D. W. Belsky, T. Huang, Accelerated biological aging and risk of depression and anxiety: Evidence from 424,299 UK Biobank participants. *Nat. Commun.* **14**, 2277 (2023).
52. D. Kwon, D. W. Belsky, A toolkit for quantification of biological age from blood chemistry and organ function test data: BioAge. *Geroscience* **43**, 2795–2808 (2021).
53. V. Codd, M. Denniff, C. Swinfield, S. C. Warner, M. Papakonstantinou, S. Sheth, D. E. Nanus, C. A. Budgeon, C. Musicha, V. Bountziouka, Q. Wang, R. Bramley, E. Allara, S. Kaptoge, S. Stoma, T. Jiang, A. S. Butterworth, A. M. Wood, E. Di Angelantonio, J. R. Thompson, J. N. Danesh, C. P. Nelson, N. J. Samani, Measurement and initial characterization of leukocyte telomere length in 474,074 participants in UK Biobank. *Nat. Aging.* **2**, 170–179 (2022).
54. C. Bycroft, C. Freeman, D. Petkova, G. Band, L. T. Elliott, K. Sharp, A. Motyer, D. Vukcevic, O. Delaneau, J. O'Connell, A. Cortes, S. Welsh, A. Young, M. Effingham, G. McVean, S. Leslie, N. Allen, P. Donnelly, J. Marchini, The UK Biobank resource with deep phenotyping and genomic data. *Nature* **562**, 203–209 (2018).
55. E. W. Diemer, J. I. Hudson, K. N. Javaras, More (adjustment) is not always better: How directed acyclic graphs can help researchers decide which covariates to include in models for the causal relationship between an exposure and an outcome in observational research. *Psychother. Psychosom.* **90**, 289–298 (2021).
56. F. Cui, Y. Sun, J. Xie, D. Li, M. Wu, L. Song, Y. Hu, Y. Tian, Air pollutants, genetic susceptibility and risk of incident idiopathic pulmonary fibrosis. *Eur. Respir. J.* **61**, 2200777 (2022).
57. M. Eeftens, R. Beelen, K. de Hoogh, T. Bellander, G. Cesaroni, M. Cirach, C. Declercq, A. Dedele, E. Dons, A. de Nazelle, K. Dimakopoulou, K. Eriksen, G. Falq, P. Fischer, C. Galassi, R. Grazuleviciene, J. Heinrich, B. Hoffmann, M. Jerrett, D. Keidel, M. Korek, T. Lanki, S. Lindley, C. Madsen, A. Molter, G. Nador, M. Nieuwenhuijsen, M. Nonnemacher, X. Pedeli, O. Raaschou-Nielsen, E. Patelarou, U. Quass, A. Ranzi, C. Schindler, M. Stempfelet, E. Stephanou, D. Sugiri, M. Y. Tsai, T. Yli-Tuomi, M. J. Varro, D. Vienneau, S. Klot, K. Wolf, B. Brunekreef, G. Hoek, Development of land use regression models for PM(2.5), PM(2.5) absorbance, PM(10) and PM(coarse) in 20 European study areas; results of the ESCAPE Project. *Environ. Sci. Technol.* **46**, 11195–11205 (2012).
58. R. Beelen, G. Hoek, D. Vienneau, M. Eeftens, K. Dimakopoulou, X. Pedeli, M.-Y. Tsai, N. Künzli, T. Schikowski, A. Marcon, K. T. Eriksen, O. Raaschou-Nielsen, E. Stephanou, E. Patelarou, T. Lanki, T. Yli-Tuomi, C. Declercq, G. Falq, M. Stempfelet, M. Birk, J. Cyrys, S. von Klot, G. Nádor, M. J. Varró, A. Dėdelė, R. Gražulevičienė, A. Mölter, S. Lindley, C. Madsen, G. Cesaroni, A. Ranzi, C. Badaloni, B. Hoffmann, M. Nonnemacher, U. Krämer, T. Kuhlbusch, M. Cirach, A. de Nazelle, M. Nieuwenhuijsen, T. Bellander, M. Korek, D. Olsson, M. Strömgren, E. Dons, M. Jerrett, P. Fischer, M. Wang, B. Brunekreef, K. de Hoogh, Development of NO_2 and NO_x land use regression models for estimating air pollution exposure in 36 study areas in Europe—The ESCAPE Project. *Atmos. Environ.* **72**, 10–23 (2013).
59. A. J. White, J. K. Kresovich, J. P. Keller, Z. Xu, J. D. Kaufman, C. R. Weinberg, J. A. Taylor, D. P. Sandler, Air pollution, particulate matter composition and methylation-based biologic age. *Environ. Int.* **132**, 105071 (2019).

Acknowledgments: We thank all the participants involved in the UK Biobank. We also thank all the staff at the UK Biobank for their contributions to this research. **Funding:** We acknowledge that we received no funding in support of this research. **Author contributions:** Conceptualization:

F.C., L.T., Y.M., J.X., B.S., Y.T., and X.Z. Writing—original draft: F.C., Y.M., B.S., and X.Z. Investigation: F.C., Y.M., B.S., and X.Z. Writing—review and editing: F.C., L.T., D.L., Y.M., B.S., and X.Z. Methodology: F.C., Y.M., J.X., B.S., and X.Z. Resources: Y.M., B.S., Y.T., and X.Z. Data curation: F.C., Y.M., B.S., Y.T., and X.Z. Validation: F.C., L.T. D.L., Y.M., B.S., Y.T., and X.Z. Formal analysis: F.C., D.L., Y.M., J.W., B.S., and X.Z. Software: F.C., Y.M., J.W., B.S., and X.Z. Visualization: F.C., Y.M., B.S., and X.Z. Supervision: Y.T. Project administration: Y.T. and X.Z. **Competing interests:** The authors declare that they have no competing interests. **Data and materials availability:** The data supporting the reported results can be found on the website of the UK Biobank (www.ukbiobank.ac.uk) upon application. The code for this study can be found in Supplementary Text 2. All other data needed to evaluate the conclusions in the paper are present in the paper and/or the Supplementary Materials.

Submitted 14 October 2023
Accepted 3 April 2024
Published 3 May 2024
10.1126/sciadv.adl3747